Journal of Sound and Vibration (2002) **258**(4), 619–631
doi:10.1006/jsvi.2002.5187, available online at http://www.idealibrary.com on IDEAL®

THE WAVE NUMBER ANALYSIS AND OPTIMAL CONTROL OF ACOUSTIC RADIATION OF A FLEXIBLE COUPLER LINK OF A LINKAGE MECHANISM

J. W. Lu, X. M. Zhang and Y. W. Shen

Mechatronic Engineering Department, Shantou University, Shantou 515063*, People's Republic of China; and Mechanical Engineering Department, Northwestern Polytechnical University, Xi'an,* 710072*, People's Republic of China*

(*Received* 10 *July* 2001, *and in final form* 11 *March* 2002)

A method for suppressing the acoustic radiation of flexible coupler link with piezoelectric elements is developed. According to the result of wave number analysis of the coupler link, it is found that not all of the components contribute to the acoustic radiation. Based on this fact, a new equation of motion the configuration of which vector directly reflect the performance of structural acoustic radiation is obtained by taking a set of transformation on the equation describing the vibration of the structure. Thus, the problem of acoustic control is successfully transformed to the problem of vibration control. Subsequently, a quadratic optimal sound radiation control method is developed, and the validity of the method is shown by some simulation results.

1. INTRODUCTION

With the development of science and technology, modern mechanisms tend to work with more high speed, while the mass tends to be more light. As a result, the mechanisms have an aptitude to vibrate when they suffer exterior excitations, and strong acoustic radiation is produced. High-speed mechanisms are widely used in industries, whose structural acoustic radiation contributes significantly to the noise pollution. So it is necessary to look for effective methods to suppress the structural acoustic radiation.

To realize the attenuation of structural acoustic radiation, one method is to attach some sound absorption materials with great damping factor in the original system [1, 2]. This method is widely used for high-frequency disturbance, but it is not effective for low-frequency disturbance. In addition, it will increase the mass of the mechanism. Another effective way is the active structural acoustic control (ASAC) method. Knyasev and Taratakvskii [3] presented this idea early in 1967, but unfortunately, it was not advanced due to the limit of relative techniques. In 1986, Taratakvskii and Vylayshev [4] presented another paper on ASAC, which provided a new feasible way to suppress structural acoustic radiation. ASAC apply secondary force to suppress the vibration of the structure so as to realize the goal of suppressing the structural acoustic radiation. ASAC can thoroughly suppress the potential of structural acoustic radiation, which overcomes the difficulty of effort to attenuate the noise in a three-dimensional sound field. Especially, in the past two decades, the technique of microprocessor has made great progress, which makes it possible to implement real-time control. Furthermore, the development of material science provides us more choice in structural acoustic control. Since Fuller *et al.*

0022-460X/02/$35.00

[5, 6] successfully apply piezoelectric actuators and sensors in the structural acoustic control in 1980s, considerable attention has been paid on the application of the smart materials in structural acoustic control. Piezoelectric transducers have the advantage of light mass, broad-frequency region, easily to be bonded to or embedded in structures, which is much convenient for placement of the apparatus of control and measurement.

Acoustic radiation are produced accompanied with the vibration of the structure, so we carry out our research based on the technique of structural vibration control. The research on the vibration control of flexible links has made a great progress in the past 20 years. Sung and Chen [7] attempted to control the elasto-dynamic response of a flexible linkage mechanism consisting of rigid crank and coupler links and a flexible follower link using piezoelectric elements as actuators and sensors. On the basis of the independent modal control method, Zhang *et al.* [8] studied the active vibration control problem for the flexible mechanisms all of whose members were considered as flexible. Recently, Zhang *et al.* [9, 10] presented a methodology for actively controlling the vibration response of high-speed flexible linkage mechanisms with bonded piezoelectric elements based on complex mode theory.

But it is a pity that there are so few papers on acoustic radiation control of flexible mechanisms. Most papers on structural acoustic radiation are restricted within the study on beams or plates with simple boundary conditions. In this paper, the wave number analysis of the structural acoustic radiation is carried out on the flexible coupler link of a flexible linkage mechanism. Based on the result of the analysis, a new equation of motion whose configuration vector directly reflects the performance of structural acoustic radiation is constructed. A quadratic optimal control method is developed. At last, simulation is implemented to verify the validity of the methodology.

2. WAVE NUMBER ANALYSIS

The system studied is a planar linkage mechanism whose crank rotates at a constant speed (Figure 1). To simplify the process of analysis, crank and follower link is assumed to be rigid, only the coupler link is flexible. Though it is a two dimensional problem for vibration analysis, the acoustic analysis is a three dimensional problem. As shown in Figure 2, the local co-ordinate of the coupler link is $OXYZ$, which moves with the link. The coupler link locates in the XY plane.

Assuming that the transverse displacement of the coupler link is obtained, it is described as follows:

$$q(x,t) = W(x)\mathrm{e}^{\mathrm{j}\omega t}, \tag{1}$$

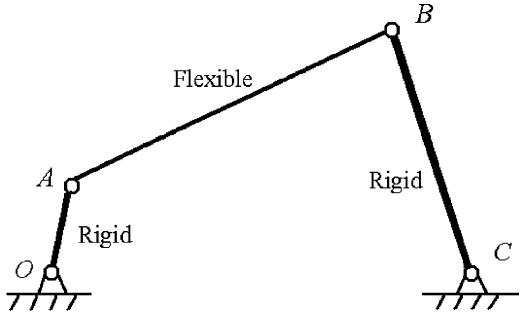

Figure 1. Crank-rocker mechanism.

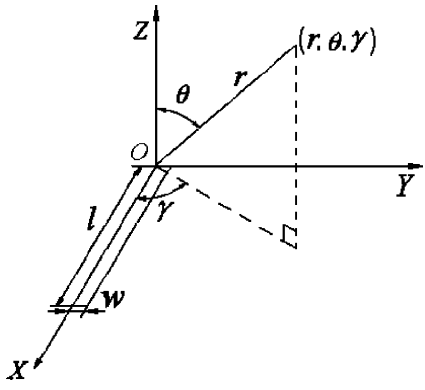

Figure 2. Local co-ordinate system.

where q is the transverse displacement of the coupler link and W is the magnitude of the displacement.

The wave number spectrum of equation (1) can be obtained by taking spatial Fourier transformation

$$\tilde{q}(k_x, t) = \int_{-\infty}^{\infty} q(x, t) \mathrm{e}^{-\mathrm{j}k_x x} \, \mathrm{d}x, \tag{2}$$

where k_x is the wave number of the coupler. According to the Euler equation [11], on the surface of the structure, the relationship between the sound field and the structure can be described as

$$\rho \frac{\partial^2 q(x, t)}{\partial t^2} = -\frac{\partial p(x, z, t)}{\partial z}\bigg|_{z=0}, \tag{3}$$

where ρ is the density of the air and p is the pressure of the sound field.

The pressure can be written as

$$p(x, z, t) = P\mathrm{e}^{\mathrm{j}(k_x x - k_z z)}\mathrm{e}^{\mathrm{j}\omega t}, \tag{4}$$

where k_z is the wave number of the sound in the z direction and $k = \omega/c$, ω is the angular frequency of the disturbance, and c is the spread speed of sound in air.

Substituting equation (4) into equation (3) yields

$$-\rho\omega^2 q(x, t) = \mathrm{j}k_z p(x, 0, t). \tag{5}$$

Equation (5) can be transformed to wave number form by spatial Fourier transformation

$$\tilde{p}(k_x, 0, t) = \frac{\mathrm{j}\rho\omega^2}{k_z} \tilde{q}(k_x, t). \tag{6}$$

The acoustic power of the coupler link is given by [12, 13]

$$\Pi = \frac{1}{T}\int_0^T \left\{ \int_L \frac{1}{2} \mathrm{Re}\left[p(x, 0, t) \frac{\partial q^*(x, t)}{\partial t} \right] \mathrm{d}L \right\} \mathrm{d}t, \tag{7}$$

where T is the period of the disturbance, the inner integral is carried out along the surface of the coupler link, the pressure and the transverse displacement can be obtained by taking inverse wave number transform into equations (2) and (6). At last, equation (7) can be

expressed as

$$\Pi = \frac{1}{T}\int_0^T \left\{ \int_0^l \frac{1}{2}\mathrm{Re}\left[\frac{1}{2\pi}\int_{-\infty}^{\infty} \frac{\mathrm{j}\rho\omega^2}{k_z}\tilde{\boldsymbol{q}}(k_x,t)\mathrm{e}^{\mathrm{j}k_x x}\,\mathrm{d}k_x \frac{-\mathrm{j}\omega}{2\pi}\int_{-\infty}^{\infty}\tilde{\boldsymbol{q}}^*(k'_x,t)\mathrm{e}^{-\mathrm{j}k'_x x}\,\mathrm{d}k'_x \right] \mathrm{d}x \right\} \mathrm{d}t. \quad (8)$$

Defining the transverse displacement $q(x,t) = 0$ out of the structure field, namely

$$q(x,t) = 0 \quad (x<0 \text{ or } x > l). \quad (9)$$

Then we can expand the integral bound from the structure surface to the whole region $(-\infty, +\infty)$, and change the sequence of integral, yielding

$$\begin{aligned}\Pi &= \frac{\rho\omega^3}{8T\pi^2}\int_0^T \left\{ \int_{-\infty}^{\infty}\int_{-\infty}^{\infty} \mathrm{Re}\left[\frac{\tilde{\boldsymbol{q}}(k_x,t)\tilde{\boldsymbol{q}}^*(k'_x,t)}{k_z} \left(\int_{-\infty}^{\infty} \mathrm{e}^{\mathrm{j}k_x x}\mathrm{e}^{-\mathrm{j}k'_x x}\,\mathrm{d}x \right) \right] \mathrm{d}k_x\,\mathrm{d}k'_x \right\} \mathrm{d}t \\ &= \frac{\rho\omega^3}{4T\pi}\int_0^T \left\{ \int_{-\infty}^{\infty} \mathrm{Re}\left[\frac{|\tilde{\boldsymbol{q}}(k_x,t)|^2}{k_z} \right] \mathrm{d}k_x \right\} \mathrm{d}t. \end{aligned} \quad (10)$$

Since in the integral field, $\gamma = 0$, then $k_z = \sqrt{k^2 - k_x^2}$, the integral above will be real only if $|k_x| \leqslant k$, then the radiated sound power can be rewritten as

$$\Pi = \frac{\rho_0\omega^3}{4T\pi}\int_0^T \left\{ \int_{-k}^{k} \frac{|\tilde{\boldsymbol{q}}(k_x,t)|^2}{\sqrt{k^2 - k_x^2}} \mathrm{d}k_x \right\} \mathrm{d}t. \quad (11)$$

The equation above reveals the fact that in the wave number spectrum of the vibration of the coupler link, only the components whose wave numbers satisfy $k_x \in [-k, k]$ have contributions to the acoustic radiation, while the rest of the components in the wave number spectrum do not have contributions to the structural acoustic radiation.

3. RECONSTRUCT THE EQUATIONS OF MOTION

The equation of motion for controlled coupler link is given by [9, 14]

$$\mathbf{M}\ddot{\mathbf{q}}(x,t) + \mathbf{C}\dot{\mathbf{q}}(x,t) + \mathbf{K}\mathbf{q}(x,t) = \mathbf{D}\mathbf{u}(t) + \mathbf{F}(t), \quad (12)$$

where $\mathbf{q}(x,t)$ is the vector of transverse displacement, $\mathbf{u}(t)$ is the vector of control force, $\mathbf{F}(t)$ is the vector of disturbance, $\mathbf{D}$ is the distribution matrix of the control force, and $\mathbf{M}$, $\mathbf{K}$, $\mathbf{C}$ are the equivalent mass, stiffness, damping matrices respectively.

According to the discussion above, the transverse displacement $\mathbf{q}(x,t)$ cannot reflect the radiated sound power directly. In the structural wave number spectrum $\tilde{\mathbf{q}}(k_x,t)$ of the coupler link, only those wave numbers $k_x \in [-k, k]$ have contributions to the acoustic radiation.

According to the expansion theorem, the transverse displacement $\mathbf{q}(x,t)$ can be rewritten as

$$\mathbf{q}(x,t) = \sum_{i=0}^{N_m} \phi_i \eta_i = \Phi\boldsymbol{\eta}, \quad (13)$$

where N_m is the number of truncated modes, Φ is the matrix including the N_m eigenvectors, $\boldsymbol{\eta}$ is the vector of modal co-ordinate. Taking wave number transformation on equation (13) yields

$$\tilde{\mathbf{q}}(k_x,t) = \int_{-\infty}^{\infty} \left(\sum_{i=0}^{N_m} \phi_i \eta_i \right) \mathrm{e}^{-\mathrm{j}k_x x}\,\mathrm{d}x = \sum_{i=0}^{N_m} \left(\int_{-\infty}^{\infty} \phi_i \mathrm{e}^{-\mathrm{j}k_x x}\,\mathrm{d}x\,\eta_i \right). \quad (14)$$

Then taking inverse wave number transformation equation (14) in the region $k_x \in [-k, k]$, one obtains

$$\begin{aligned}\mathbf{p}(x,t) &= \int_{-k}^{k}\left[\sum_{i=0}^{N_m}\left(\int_{-\infty}^{\infty}\phi_i e^{-jk_x x}\,dx\eta_i\right)\right]e^{jxk_x}\,dk_x \\ &= \sum_{i=0}^{N_m}\left[\int_{-k}^{k}\left(\int_{-\infty}^{\infty}\phi_i e^{-jk_x x}\,dx\eta_i\right)e^{jxk_x}\,dk_x\right] \\ &= \sum_{i=0}^{N_m}\left[\int_{-k}^{k}\left(\int_{-\infty}^{\infty}\phi_i e^{-jk_x x}\,dx\right)e^{jxk_x}\,dk_x\eta_i\right]. \end{aligned} \tag{15}$$

Defining

$$\psi_i = \int_{-k}^{k}\left(\int_{-\infty}^{\infty}\phi_i e^{-jk_x x}\,dx\right)e^{jxk_x}\,dk_x \quad (i = 1, 2, \ldots, N_m). \tag{16}$$

Substituting equation (16) into equation (15), yields

$$\mathbf{p}(x,t) = \sum_{i=0}^{N_m}\psi_i\eta_i = \Psi\boldsymbol{\eta}, \tag{17}$$

where Ψ is a matrix including N_m number of vectors ψ_i $(i = 1, 2, \ldots, N_m)$.

Pre-multiplying equation (13) with $\Phi^{\mathrm{T}}\mathbf{M}$ yields

$$\boldsymbol{\eta} = \Phi^{\mathrm{T}}\mathbf{M}\mathbf{q}. \tag{18}$$

Substituting equation (18) into equation (17) yields

$$\mathbf{p} = \Psi\boldsymbol{\eta} = \Psi\Phi^{\mathrm{T}}\mathbf{M}\mathbf{q}. \tag{19}$$

Define the transformation matrix by

$$\mathbf{W} = \Psi\Phi^{\mathrm{T}}\mathbf{M}. \tag{20}$$

Then equation. (19) can be rewritten as

$$\mathbf{p} = \mathbf{W}\mathbf{q}. \tag{21}$$

For a given position of the crank, the modal matrix Φ is known, so Φ and $\mathbf{W} = \Psi\Phi^{\mathrm{T}}\mathbf{M}$ are also known.

Making the following transformations

$$\mathbf{M} = (\mathbf{M}\mathbf{W}^{-1})\mathbf{W} = \mathbf{M}_e\mathbf{W}, \qquad \mathbf{C} = (\mathbf{C}\mathbf{W}^{-1})\mathbf{W} = \mathbf{C}_e\mathbf{W}, \tag{22a, b}$$

$$\mathbf{K} = (\mathbf{K}\mathbf{W}^{-1})\mathbf{W} = \mathbf{K}_e\mathbf{W}, \tag{22c}$$

Substituting equation (22) into equation (12), yields

$$\mathbf{M}_e\mathbf{W}\ddot{\mathbf{q}}(x,t) + \mathbf{C}_e\mathbf{W}\dot{\mathbf{q}}(x,t) + \mathbf{K}_e\mathbf{W}\mathbf{q}(x,t) = \mathbf{D}\mathbf{u}(t) + \mathbf{F}(x,t). \tag{23}$$

Substituting equation (21) into equation (23), a new equation is obtained:

$$\mathbf{M}_e\ddot{\mathbf{p}}(x,t) + \mathbf{C}_e\dot{\mathbf{p}}(x,t) + \mathbf{K}_e\mathbf{p}(x,t) = \mathbf{D}\mathbf{u}(t) + \mathbf{F}(x,t). \tag{24}$$

In equation (24), $\mathbf{p}$ can be regarded as a measure of the acoustic radiation power. Namely, the acoustic radiation power will decrease as long as the value of $\mathbf{p}$ is suppressed. So it is more convenient to study the acoustic radiation control using equation (24). In other words, the acoustic radiation control problem is transformed to the vibration control problem.

4. THE QUADRATIC OPTIMAL CONTROL

A set of new eigenvalues ω_{ei} $(i = 1, 2, \ldots, N_m)$ and corresponding eigenvectors φ_i $(i = 1, 2, \ldots, N_m)$ can be obtained by solving the homogeneous equation of equation (24). $\mathbf{p}$ can be described with φ_i as follows:

$$\mathbf{p}(x, t) = \sum_{i=0}^{N_m} \varphi_i \mu_i = \boldsymbol{\varphi}\boldsymbol{\mu}. \tag{25}$$

Assuming that the eigenvectors φ_i are normalized vectors, we have

$$\boldsymbol{\varphi}^{\mathrm{T}}\mathbf{M}_e\boldsymbol{\varphi} = I, \qquad \boldsymbol{\varphi}^{\mathrm{T}}\mathbf{K}_e\boldsymbol{\varphi} = \boldsymbol{\Omega}_e^2. \tag{26a, b}$$

Substituting equation (25) into equation (24) and pre-multiplying by $\boldsymbol{\varphi}^{\mathrm{T}}$, with the proportional viscous damping assumption, equation (24) can be decoupled as

$$\ddot{\boldsymbol{\mu}} + 2\boldsymbol{\zeta}_e\boldsymbol{\Omega}_e\dot{\boldsymbol{\mu}} + \boldsymbol{\Omega}_e^2\boldsymbol{\mu} = \boldsymbol{\varphi}^{\mathrm{T}}\mathbf{D}\mathbf{u} + \boldsymbol{\varphi}^{\mathrm{T}}\mathbf{F}. \tag{27}$$

Equation (27) can be rewritten in the form of state space as follows [9, 14]:

$$\dot{\mathbf{x}} = \mathbf{A}\mathbf{x} + \mathbf{B}\mathbf{f}, \tag{28}$$

where

$$\mathbf{x} = \begin{bmatrix} \boldsymbol{\mu} \\ \dot{\boldsymbol{\mu}} \end{bmatrix}, \quad \mathbf{A} = \begin{bmatrix} \mathbf{0} & \mathbf{I} \\ -\mathbf{Y} & -\mathbf{Z} \end{bmatrix}, \quad \mathbf{B} = \begin{bmatrix} \mathbf{0} \\ \mathbf{I} \end{bmatrix},$$

$$\mathbf{f} = \mathbf{f}_{ctr} + \mathbf{f}_{ext}, \quad \mathbf{f}_{ctr} = \boldsymbol{\varphi}^{\mathrm{T}}\mathbf{D}\mathbf{u}, \quad \mathbf{f}_{ext} = \boldsymbol{\varphi}^{\mathrm{T}}\mathbf{F},$$

$$\mathbf{Y} = \begin{bmatrix} \ddots & & \\ & \omega_{ei}^2 & \\ & & \ddots \end{bmatrix}, \quad \mathbf{Z} = \begin{bmatrix} \ddots & & \\ & 2\zeta_{ei}\omega_{ei} & \\ & & \ddots \end{bmatrix},$$

where ζ_{ei} is the new ith modal damping factor.

Typically, not all of the N_m modes need to be controlled, so the design problem can be truncated. To this end, we partition the N_m modes into N_c controlled modes and N_r residual modes. Accordingly, the state vector $\mathbf{x}$ can be partitioned into two parts:

$$\mathbf{x} = \begin{bmatrix} \mathbf{x}_c \\ \mathbf{x}_r \end{bmatrix}, \tag{29}$$

where

$$\mathbf{x}_c = \begin{bmatrix} \boldsymbol{\mu}_c \\ \dot{\boldsymbol{\mu}}_c \end{bmatrix}, \quad \mathbf{x}_r = \begin{bmatrix} \boldsymbol{\mu}_r \\ \dot{\boldsymbol{\mu}}_r \end{bmatrix},$$

$\boldsymbol{\mu}_c$ is the modal co-ordinates of the controlled modes, $\boldsymbol{\mu}_r$ is the modal co-ordinates of the residual modes.

Accordingly, $\mathbf{f}_{ctr}$ is also partitioned into two parts:

$$\mathbf{f}_{ctr} = \begin{bmatrix} \mathbf{f}_c \\ \mathbf{f}_r \end{bmatrix}, \tag{30}$$

where $\mathbf{f}_c$ is the modal control force vector of controlled modes, while $\mathbf{f}_r$ is the modal control force vector of residual modes, and $\mathbf{f}_c$ is given by

$$\mathbf{f}_c = \boldsymbol{\varphi}_c^{\mathrm{T}}\mathbf{D}\mathbf{u}. \tag{31}$$

For linear feedback of the controlled modes, the control law is [14, 15]

$$\mathbf{f}_c = \begin{bmatrix} f_1 \\ f_2 \\ \vdots \\ f_{N_c} \end{bmatrix} = -\mathbf{G}x = -\mathbf{G}_1\boldsymbol{\mu}_c - \mathbf{G}_2\dot{\boldsymbol{\mu}}_c, \tag{32}$$

where

$$\mathbf{G} = \begin{bmatrix} \mathbf{G}_1 & \\ & \mathbf{G}_2 \end{bmatrix},$$

$$\mathbf{G}_1 = \begin{bmatrix} g_{11} & & & & \\ & \ddots & & & \\ & & g_{1i} & & \\ & & & \ddots & \\ & & & & g_{1N_c} \end{bmatrix}, \quad \mathbf{G}_2 = \begin{bmatrix} g_{21} & & & & \\ & \ddots & & & \\ & & g_{2i} & & \\ & & & \ddots & \\ & & & & g_{2N_c} \end{bmatrix}.$$

Introducing the following quadratic performance index:

$$\begin{aligned} J &= \frac{1}{2}\int_{t_1}^{t_2} (\mathbf{x}^{\mathrm{T}}\mathbf{Q}\mathbf{x} + \mathbf{f}_c^{\mathrm{T}}\mathbf{R}\mathbf{f}_c)\,\mathrm{d}t \\ &= \frac{1}{2}\sum_{i=1}^{N_c}\int_{t_1}^{t_2} (\omega_{ei}^2\mu_i^2 + \dot{\mu}_i^2 + r_i f_i^2)\,\mathrm{d}t, \end{aligned} \tag{33}$$

$$\mathbf{Q} = \begin{bmatrix} \omega_{e1}^2 & & & & & & \\ & \ddots & & & & & \\ & & \omega_{ei}^2 & & & & \\ & & & \ddots & & & \\ & & & & \omega_{eN_c}^2 & & \\ & & & & & 1 & \\ & & & & & & \ddots \\ & & & & & & & 1 \end{bmatrix}_{2N_c\times 2N_c}, \quad \mathbf{R} = \begin{bmatrix} r_1 & & & & \\ & \ddots & & & \\ & & r_i & & \\ & & & \ddots & \\ & & & & r_{N_c} \end{bmatrix}_{N_c\times N_c},$$

where $\mathbf{Q}$ is a positive-definite weighing matrix, $\mathbf{R}$ is a semi-definite weighing matrix.

In equation (33), the first term denotes the potential energy of the ith mode, the second term denotes the kinetic energy of the ith mode, and the third term denotes the energy expanded by the ith modal control force.

Using modal control theorem [12], the optimal modal control force $\mathbf{f}_c$ can be obtained by maximum theorem, and the ith modal gain is given by

$$g_{1i} = \omega_{ei}\sqrt{\omega_{ei}^2 + r_i^{-1}} - \omega_{ei}^2, \quad g_{2i} = \sqrt{r_i^{-1} + 2g_{1i}}. \tag{34a, b}$$

According to equation (31), the control force output of the actuators can be written as

$$\mathbf{u} = (\boldsymbol{\Phi}_c^{\mathrm{T}}\mathbf{D})^{-1}\mathbf{f}_c. \tag{35}$$

5. FEEDBACK CONTROLLER

It should be noted that in the above analysis, $\mathbf{f}_c$ is the function of modal displacement $\boldsymbol{\mu}_c$ and modal velocity $\dot{\boldsymbol{\mu}}_c$, while it is impossible to measure $\boldsymbol{\mu}_c$ and $\dot{\boldsymbol{\mu}}_c$ directly. In addition, the above analysis is carried out based on equation (24). It is necessary to describe $\mathbf{f}_c$ in the form of general co-ordinate vector $\mathbf{q}(x,t)$, which can be directly measured. In other words, we should find out the relationship between $\mathbf{q}(x,t)$ and the parameters $\boldsymbol{\mu}_c$ and $\dot{\boldsymbol{\mu}}_c$.

At present, piezoelectric elements are widely used as actuators and sensors, the output of piezoelectric sensors are related with the deformation of structure plant. Here, we use proportional–differential (PD) controller as the feedback controller to implement quadratic optimal control. It is necessary to find the relationship between the gains of the PD controller and the modal control gains given by equation (34).

Substituting equation (21) into equation (25) yields

$$\mathbf{W}\mathbf{q} = \boldsymbol{\varphi}\boldsymbol{\mu}. \tag{36}$$

Pre-multiplying the above equation by $\mathbf{W}^{-1}$, one obtains

$$\mathbf{q} = \mathbf{W}^{-1}\boldsymbol{\varphi}\boldsymbol{\mu}. \tag{37}$$

Assuming that the number of the piezoelectric sensor is m, then the control force is given by

$$\mathbf{F}_{ctr} = \mathbf{D}\mathbf{u} = \sum_{j=1}^{m}\left(K_{lj} + K_{dj}\frac{\mathrm{d}}{\mathrm{d}t}\right)\mathbf{H}_j\mathbf{q}\mathbf{F}_{ctr} = \mathbf{D}\mathbf{u} = \sum_{j=1}^{m}\left(K_{lj} + K_{dj}\frac{\mathrm{d}}{\mathrm{d}t}\right)\mathbf{H}_j\mathbf{q}, \tag{38}$$

where K_{lj}, K_{dj} are proportional and differential gains, respectively, $\mathbf{H}_j$ is the relationship matrix between the jth sensor and the displacement of the structure nodes.

The modal control force of the N_c controlled modes can be expressed as

$$\mathbf{f}_c = \boldsymbol{\varphi}_c^{\mathrm{T}}\mathbf{D}\mathbf{u} = \boldsymbol{\varphi}_c^{\mathrm{T}}\mathbf{F}_{ctr} = \boldsymbol{\varphi}_c^{\mathrm{T}}\sum_{j=1}^{m}\left(K_{lj} + K_{dj}\frac{\mathrm{d}}{\mathrm{d}t}\right)\mathbf{H}_j\mathbf{W}^{-1}\boldsymbol{\varphi}\boldsymbol{\mu}. \tag{39}$$

Properly selecting the gains K_{lj} and K_{dj}, the follwing equations can be satisfied:

$$\{\boldsymbol{\varphi}_i\}^{\mathrm{T}}\sum_{j=1}^{m}K_{lj}\mathbf{H}_j\mathbf{W}^{-1}\{\boldsymbol{\varphi}_k\} = \begin{cases} g_{1i}, & i = k \\ 0, & i \neq k \end{cases} \quad (i,k = 1,2,\ldots,N_c), \tag{40a}$$

$$\{\boldsymbol{\varphi}_i\}^{\mathrm{T}}\sum_{j=1}^{m}K_{dj}\mathbf{H}_j\mathbf{W}^{-1}\{\boldsymbol{\varphi}_k\} = \begin{cases} g_{2i}, & i = k \\ 0, & i \neq k \end{cases} \quad (i,k = 1,2,\ldots,N_c). \tag{40b}$$

Then the control will achieve the effort of the optimal controller described above. Equation (40) can be rewritten as

$$\mathbf{H}\mathbf{W}^{-1}\{\bar{\mathbf{K}}_l\} = \{\mathbf{g}_1\}, \quad \mathbf{H}\mathbf{W}^{-1}\{\bar{\mathbf{K}}_d\} = \{\mathbf{g}_2\}, \tag{41a, b}$$

where $\mathbf{H} = [\mathbf{H}_1 \ \cdots \ \mathbf{H}_m]^{\mathrm{T}}$, $\{\bar{\mathbf{K}}_l\} = \{K_{l1} \ \cdots \ K_{lm}\}^{\mathrm{T}}$, $\{\bar{\mathbf{K}}_d\} = \{K_{d1} \ \cdots \ K_{dm}\}^{\mathrm{T}}$, and $\{\mathbf{g}_1\} = \{g_{11} \ \cdots \ g_{1N_c}\}^{\mathrm{T}}$, $\{\mathbf{g}_2\} = \{g_{21} \ \cdots \ g_{2N_c}\}^{\mathrm{T}}$.

The gains of the PD controller is given by

$$\{\bar{\mathbf{K}}_l\} = (\mathbf{H}\mathbf{W}^{-1})^{-1}\{\mathbf{g}_1\}, \quad \{\bar{\mathbf{K}}_d\} = (\mathbf{H}\mathbf{W}^{-1})^{-1}\{\mathbf{g}_2\}. \tag{42a, b}$$

If $N_c = m$, then $(\mathbf{H}\mathbf{W}^{-1})^{-1}$ is the inverse matrix of $\mathbf{H}\mathbf{W}^{-1}$, otherwise $(\mathbf{H}\mathbf{W}^{-1})^{-1}$ is the general inverse matrix of $\mathbf{H}\mathbf{W}^{-1}$.

6. SIMULATION AND RESULTS

In order to verify the validity of the proposed control methodology, a computer simulative analysis is carried out on a mechanism shown in Figure 1. The crank and follower link is rigid, only the coupler link is flexible. The structural parameters of the mechanism are listed in Table 1, material parameters are listed in Table 2. A pair of actuators and a pair of sensors are bonded on the coupler link. The actuators are manufactured from piezoelectric ceramic with thickness 0·5 mm, and the sensors from piezoelectric polymer with thickness 0·2 mm. The two actuators are located at one- and three-fourth of the length of the coupler link respectively. In this study, the coupler link is modelled by 12 finite elements. The crank speed is 600 r.p.m. The first six modes are used to calculate the response of the system while the first three modes are taken as controlled modes, i.e., $N_c = 3$ and $N_r = 3$. The results of the simulation are shown in Figures 3–7.

Figure 3 shows the optimal control force in a cycle of motion of the mechanism, in which solid curve is the output of the actuator near the crank, and the dashed one is the output of the actuator near the follower link. Since the excitation is transferred from crank to coupler link and follower link, the output of the actuator near the crank is greater than that of the other actuator.

Figure 4 shows the control voltage in a cycle of motion of the mechanism. The solid curve is the voltage implemented on the actuator near the crank, and the dashed one is that implemented on the actuator near the follower link. Since the voltage is linear to the control force, the shape of these two curves is similar to the two curves shown in Figure 3.

TABLE 1

Size parameters of the mechanism

Parameters	*OA*	*AB*	*BC*	*OC*
Length (m)	0·1	0·48	0·4	0·4
Width (m)	0·048	0·048	0·048	—
Thickness (m)	0·005	0·005	0·005	—

TABLE 2

Material parameters of the mechanism

Parameters	*Plant*	*Piezoelectric actuators*	*Piezoelectric sensors*
Young's modulus (N/m^2)	$7{\cdot}102 \times 10^{10}$	$1{\cdot}17 \times 10^{11}$	$0{\cdot}15 \times 10^{10}$
Poisson's coefficient	0·25	0·25	0·25
Volumetric density (kg/m^3)	2712	7500	1760

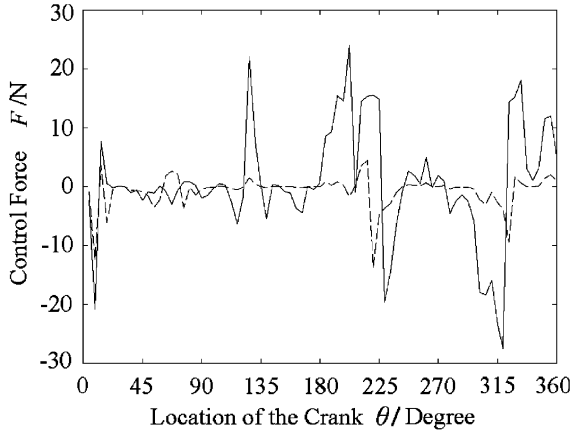

Figure 3. The optimal control force.

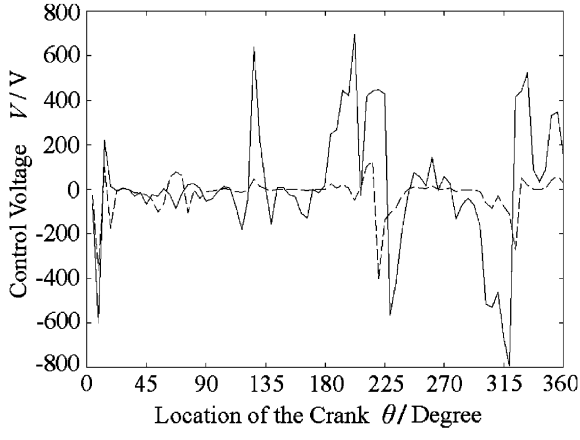

Figure 4. The control voltage.

It should be noted that, a certain piezoelectric ceramic actuator can only stand voltage in a certain region, when the voltage implemented exceeds this region, the actuator will lapse.

Figure 5 shows the comparison of the wave number spectrum of the structural vibration while the crank is located at $\theta = 90^{\circ}$. Similar results can be also be obtained when the crank is located in other locations. In this study, the acoustic wave number is $k = \omega/c = 0{\cdot}185$. It can be seen that the components that satisfy $k_x < k$ in the wave number spectrum are suppressed after control.

Figure 6 shows the comparison of the radiated sound power in one cycle of operation with and without control. The solid curve shows the acoustic power level without control, and the dashed curve is that with control. It is seen that the radiated sound power is successfully suppressed after the control force is applied.

Figure 7 shows the comparison of the sound pressure at a certain point in one cycle of operation with and without control. The point studied is located at $r = 1{\cdot}20$ m, $\theta = 20^{\circ}$, $\gamma = 0^{\circ}$ (the meaning of the parameters is shown in Figure 2). The solid curve is the sound

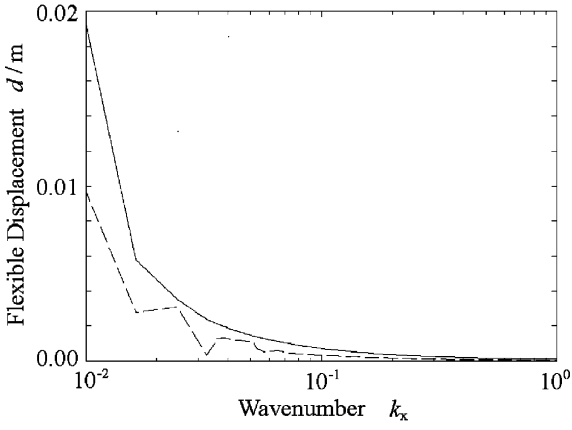

Figure 5. Comparison of the vibration wave number spectrum with and without control.

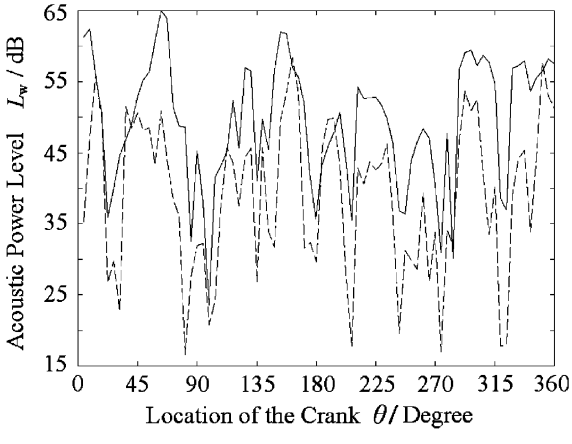

Figure 6. Comparison of the radiated sound power with and without control.

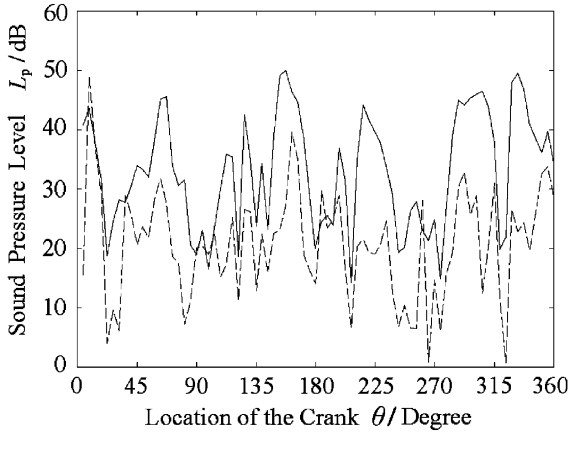

Figure 7. Comparison of the sound pressure with and without control.

pressure without control, and the dashed one is that with control. It is seen that the sound pressure at the point is attenuated after the control force is applied. The maximum of the sound pressure at this point is decreased by about 15 dB after control.

7. CONCLUSION

In this paper, wave number analysis of the structural acoustic radiation is carried out on the flexible coupler link of a linkage mechanism. The result reveals that in the wave number spectrum of structural vibration of the coupler link, only those wave number $k_x \in [-k, k]$ have contributions to the acoustic radiation, while the rest components in the wave number spectrum do not have contributions to the structural acoustic radiation. Based on this result, a new equation of motion whose configuration vector directly reflects the radiated sound power is presented. On the basis of the new equation, a quadratic optimal sound radiation control method is developed. Simulation results show that the method presented is valid.

ACKNOWLEDGMENTS

This research was supported by the National Natural Science Foundation of China under grants 59975056 and 59605001, the Natural Science Foundation of Guangdong Province under grants 20000783 and 97031, the Foundation for University Key Teacher by the Ministry of Education of China and Guangdong Province. The second author gratefully acknowledges these supports.

REFERENCES

1. X. M. Zhang 1999 *Chinese Journal of Mechanical Engineering* **35**, 55–58. Modal loss factor predication in the passive vibration control of elastic mechanism systems.
2. X. M. Zhang and A. G. Erdman 2001 *Computers and Structures* **79**, 1265–1274. Dynamic response of flexible linkage mechanisms with viscoelastic constrained layer damping treatment.
3. A. S. Knyasev and B. D. Taratakvskii 1967 *Soviet Physics Acoustics* **13**, 115–117. Abtement of radiation from flexurally vibration plates by means of active local dampers.
4. B. D. Taratakvskii and A. L. Vylayshev 1986 *Soviet Physics Acoustics* **32**, 96–98. Active acoustic reduction of plate.
5. C. R. Fuller, C. A. Rogers and H. H. Robertshaw 1989 *Proceedings of SPIE Conference on Fiber Optic Smart Structures and Skins II, Boston, MA*, 1170, 338–358. Active structural acoustic control with smart structure.
6. E. K. Dimitriadis, C.R. Fuller and C. A. Rogers 1991 *American Society of Mechanical Engineers Journal of Vibration and Acoustic* **113**, 21–28. Piezoelectric actuators for distributed excitation of thin plates.
7. C. K. Sung and Y. C. Chen 1991 *American Society of Mechanical Engineers Journal of Vibration and Acoustics* **113**, 14–21. Vibration control of the elastodynamic response of high-speed flexible linkage mechanisms.
8. X. M. Zhang, H. Z. Liu and W. Q. Cao 1996 *Chinese Journal of Mechanical Engineering* **32**, 7–14. Active vibration control of flexible mechanisms.
9. X. M. Zhang, C. J. Shen and Y. W. Shen 2000 *Journal of Sound and Vibration* **234**, 491–506. Complex mode active vibration control of high-speed flexible linkage Mechanisms.
10. X. M. Zhang, C. Shao, S. Li, D. Xu and A. G. Erdman 2001 *Journal of Sound and Vibration* **243**, 145–155. Robust H_∞ vibration control for flexible linkage mechanism systems with piezoelectric sensors and actuators.
11. M. P. Norton 1993 *Fundamentals of Noise and Vibration Analysis for Engineers*. Beijing: Aviation Industry Press (Chinese version).

12. R .L. Clark and C. R. Fuller 1991 *Proceedings of the Conference on Recent Advances in Active Control of Sound and Vibration, Blacksburg, VA*, 507–524. Active structural acoustic control with adaptive structures including wave number considerations.
13. S. Sommerfeldt 1993 *Proceedings of the 2nd Conference on Recent Advances in Active Control of Sound and Vibration, Blacksburg, VA,* 929–940. Active wave number control of acoustic radiation from a plate.
14. R. A. Canfield and L. Meirovitch 1994 *American Institute of Aeronautics and Astronautics Journal* **32**, 2053–2060. Integrated structural design and vibration suppression using independent modal space control.
15. C. R. Fuller, S. J. Eliott and P. A. Nelson 1996 *Active Control of Vibration*. London: Academic Press.